euronoise

Photoacoustic metrology of nanoimprint polymers

Timothy Kehoe[a], Juerg Bryner[b], Jacqueline Vollmann[b], Clivia Sotomayor Torres[a], Laurent Aebi[b] and Juerg Dual[b]

[a]Tyndall National Institute, Lee Maltings, University College Cork, Prospect Row, Cork, Ireland
[b]ETH Zurich, Institute of Mechanical Systems, Dept. of Mechanical and Process Engineering, CH 8092 Zurich, Switzerland
tim.kehoe@tyndall.ie

Nanoimprint lithography (NIL) is an alternative lithography method for patterning of thin polymer films using a rigid stamp, which is being developed as desired minimum feature sizes reduce to the scale of tens of nanometres. To characterise nanoimprinted structures, there is a need for more convenient and non-destructive wafer-scale metrologies to complement scanning electron microscopy and atomic force microscopy. The photoacoustic method, with a resolution in the range of 10 nm, and normally used to measure metal and dielectric layer thicknesses and physical properties, has been used for the first time to study nanoimprinting polymer layers. A good signal was obtained from the top and the bottom interfaces of two polymers, mr-I PMMA 75k300 and mr-NIL 6000.3, with thicknesses ranging from 100 to 500 nm. From the measured time of flight of the acoustic wave, and modelling physical parameters of the polymers, thicknesses calculated agree well with those measured by profilometry. The measurements are performed on a short pulse laser pump-probe setup, where bulk wave packets are excited and detected using near infrared laser pulses of less than 100 fs duration. The entire experimental setup is simulated numerically. The resonant acoustic signal from patterned polymer layers was also simulated.

1 Introduction

Nanoimprint lithography (NIL), first demonstrated in 1995 [1], is routinely used to imprint features with dimensions close to or smaller than 50 nm [2], with 6 nm printing being demonstrated over small areas of several hundred micrometres length [3]. Imprinting of features of less than 50 nm has been studied on wafers of diameter up to 300 mm [4]. In the quest to control and standardise the NIL process, and to make the transfer of imprinting sub-50 nm features over small areas up to wafer scale, it is necessary to characterise the quality of these imprints in terms of their critical dimension and height in order that devices fabricated by NIL perform to their designed specifications.

Applications ranging from patterning resist layers for semiconductor processing or using the imprinted polymers themselves depend upon very accurate reproduction of spatial patterns and dimensions. It is essential to compare process parameters such as temperature and pressure, equipment and materials, in terms of imprint quality. In an industrial environment, continuous data acquisition related to pattern reproduction quality is necessary to maintain yield and highlight sources of defects and failures, and this requires more convenient wafer-scale characterisation methods.

Existing microscopy methods have various strengths in terms of looking at features in the nanoscale, but they also each display particular drawbacks. To look below the diffraction limit of optical microscopy, about 200 nm, the most routinely used method is scanning electron microscopy (SEM), which distinguishes features below 1 nm [5]. However, such very high resolution is limited to a very small field of view, and is relatively time-consuming to obtain. Another limitation of SEM is the need to cleave or cross-section samples to obtain information about their height.

Atomic force microscopy (AFM) and other scanning probe methods also have very high resolutions. In the case of AFM, this is almost at the atomic scale [6], but again with a concomitant small scanning area. Scanning near-field optical microscopy can resolve features as small as 50 nm, using optical wavelengths [7]. However, scanning methods are limited in speed since an image is built up by the probe crossing the surface serially.

Scatterometry makes use of changes in the polarisation or angular intensity of optical wavelengths of light to provide information about structures below the diffraction limit [8]. However, it requires a very accurate value of the complex refractive index of the patterned layer. Recently sub-wavelength diffraction has been demonstrated as a means of characterising nanoscale features [9].

Photoacoustic metrology can provide high resolution measurements of layer thicknesses, with resolution in the range of 10nm [10] if short wavelength phonons are used, but until now the method has been used mainly to characterise metal and dielectric materials. We demonstrate its use to study nanoimprint polymers at the nanoscale, by recording the signal from the interface of 100 nm – 500 nm thick layers with aluminium and silicon, using a femtosecond laser pump probe setup. The entire experimental setup is simulated numerically, and the laser acoustic measurements are compared with profilometry measurements performed on the same thin film structures in order to quantify the dimensions and mechanical properties of the polymer films.

The photoacoustic signal from imprinted polymer structures has been simulated using finite element methods. Results show that signals due to acoustic resonant modes of 50 nm scale structures are of a frequency range that is measurable by photoacoustic metrology.

2 Method

The laser acoustic method introduced by Thomsen et al. [11] is well known and widely used in the semiconductor industry, mostly for measurements on metallic specimens, e.g. interconnects of computer chips. Here, the thicknesses of two printable polymers, mr-I PMMA 75k300 and mr-NIL 6000.3, ranging from 100 to 600 nm, were measured and compared to values obtained by profilometry. The current measurements are performed with a pump probe setup (Figure 1 (a)) which is described by Vollmann et al. [10]. The laser beam (pulses <100 fs, repetition rate 81 MHz, wavelength 800 nm) is split into a pump and a probe beam for the excitation and the detection, respectively.

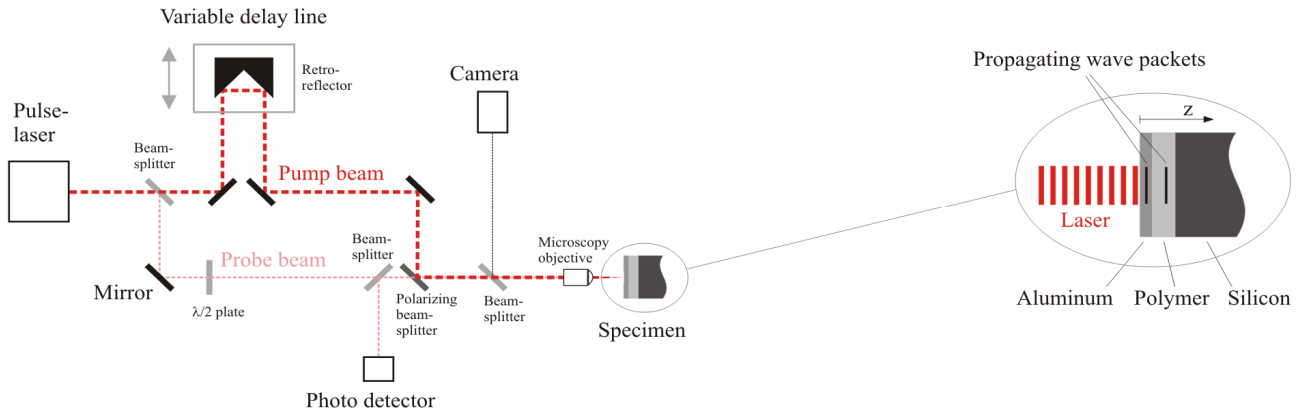

Figure 1 (a) Main components of the experimental setup. (b) Structure of the specimens: Aluminum layer (60 nm), polymer layer (100-600 nm), silicon wafer.

At the surface of the specimen the pump pulse generates stress which starts to propagate mainly as one-dimensional bulk wave packet into the specimen. The absorption depth of the laser in the surface defines the average wavelength, and therefore the resolution of the method, and this is less than 20 nm for aluminium. At every interface of the layered specimen the waves are partly reflected, thus heading back to the surface. Near the surface, the wave packets cause a small change of the optical reflectivity due to the photoacoustic effect.

The optical reflectivity is recorded with a photo-detector that measures the intensity of the reflected probe beam. With this procedure the time of flight of the wave packets through the thin film layers is measured. If the material properties determining the bulk wave velocity are known, with the measured time of flight the thickness of the corresponding layer can be determined. Or vice versa, for a known thickness, the bulk wave velocity can be determined, and from this the physical parameters such as Young's modulus and Poisson's ratio may be determined.

Numerical simulations are performed for a full interpretation of the measurements presented in the next section. The simulations are calculated with a one-dimensional simulation model consisting of three main parts which are shown in Fig. 2. In the first part the temperature distribution in the top metal layer heated by the laser pulse is calculated with a two temperature model described by Qiu et al. [12]. The propagation of the wave packets is calculated in the second part of the simulation using a visco-elastic material model, providing the temporal and lateral distribution of strain and stress in the specimen. In the third part the photoacoustic effect, i.e. the optical reflectivity change at the surface $\Delta R(t)$ is calculated. $\Delta R(t)$ depends on the so called sensitivity function $F(z)$ (see Thomsen et. al. [11]) and the strain distribution $\varepsilon(z, t)$.

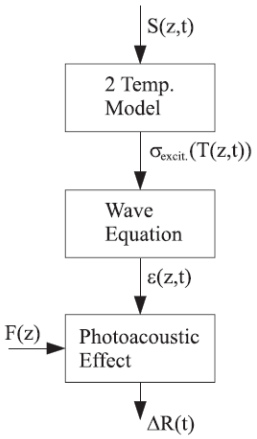

Figure 2. Simulation model: laser power density S, excited stress σ_{excit}, temperature T, spatial coordinate z, strain ε, sensitivity function F(z), and optical reflectivity change ΔR.

3 Results

Figure 3(a) shows a measurement of an Al/PMMA/Si specimen. The thickness of the PMMA layer is determined by profilometry to be 336 nm. The first vertical dashed line denotes the arrival time of the first wave packet heading back to the surface, 20.3 ps. This is the roundtrip time for wave packets in the aluminum layer. Taken from the literature, the bulk wave velocity of aluminum is assumed to be 6362 m/s. With this value and the roundtrip time the thickness of the aluminum layer is determined to be 64.6 nm.

In order to interpret all peaks of the measurement, the simulation of the stress field is considered in Figure 3(b). At time zero at the surface of the aluminum layer the pump pulse arrives and launches a wave packet. After 10.15 ps the wave packet arrives at the interface Al/PMMA. One part of the packet is reflected and one part is transmitted into the PMMA. After 20.3 ps the first wave packet returns to the surface (first red circle), then every 20.3 ps another wave packet arrives at the surface. After 284.9 ps the first wave packet that traveled through the PMMA arrives back at the surface (first green circle). The roundtrip time through the PMMA is given by the difference of this arrival and the arrival of the first reflection after 20.3 ps: Δt PMMA = 264.6ps.

This roundtrip time together with the measured thickness of 336 nm of the PMMA layer by profilometry leads to the bulk wave velocity of 2540 m/s. Velocities of 2577 m/s and 2675 m/s are measured for a 125 nm and a 586 nm PMMA specimen, respectively. For five different mr-L 6000.3 XP specimens 2500 m/s ±3% are measured.

Using values provided by the manufacturers for the Poisson's ratio and density, of 0.4 (for both polymers), and 1012 kgm^{-3} and 1008 kgm^{-3} for mr-IPMMA and mr-NIL6000 respectively, the values of Young's modulus calculated from the acoustic speeds are 3.20 GPa and 2.95 GPa. Conversely, if the physical parameters of the polymer are already known, then from the time of flight data, the dimensions of the polymers may be known with the same accuracy.

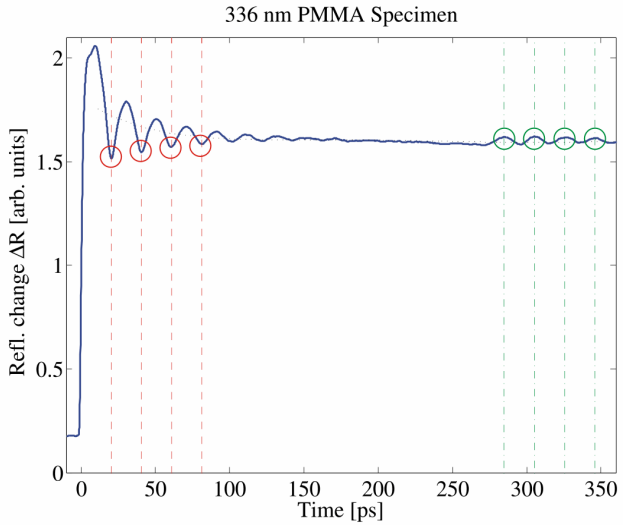

Figure 3 (a). Measured reflectivity change in a Al/PMMA/Si specimen.

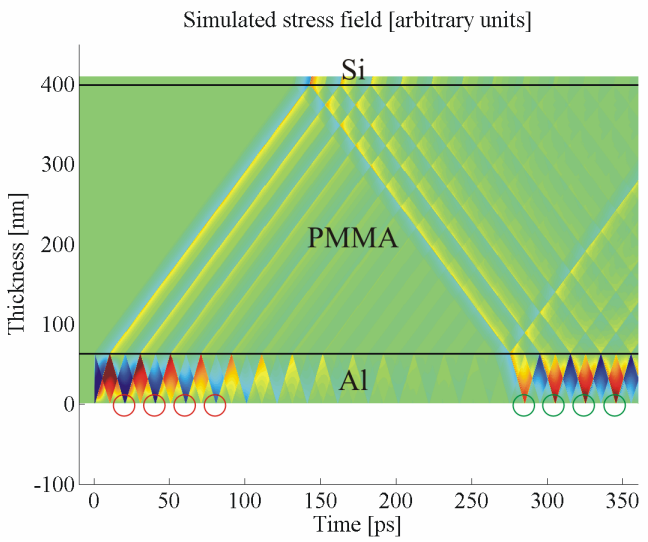

Figure 3 (b). Simulated stress field of the same Al/PMMA/Si specimen: Excitation at time zero, signal from reflections of the wave packet at the interface Al/PMMA denoted by red circles, signal from reflections of the wave packet at the interface PMMA/Si denoted by green circles.

3.1 Confined acoustic resonant modes

The depth resolution of photoacoustic metrology is only limited by the wavelength of the acoustic wave packet generated at the light-absorbing surface, which is less than 20 nm. However, the lateral resolution is limited by the ability to focus the excitation light-source, and so is approximately 0.5 µm. As a means to characterise imprinted polymer layers of structures with widths as small as 50 nm, the acoustic resonant modes of sets of imprinted lines were studied by finite element simulations. Previously it has been found that metallic nanostructures have displayed a photoacoustic signal in the GHz range, dependant on modes which are characteristic of their size and material properties [13].

It was found that polymer lines have vibrational resonances related to their width and height in the GHz scale (see Table 1). These modes may be excited by a photoacoustic probe beam and are within the range of detection of the photoacoustic metrology apparatus, adding a component to the photoacoustic signal with a period in the range of hundreds of picoseconds. The structures studied were gratings of equal line and spacing widths of 50 nm, 100 nm and 200 nm and height 100 nm. Simulations were performed of cross-sections of the lines to reduce computation times, so that the vibrational modes obtained are due to oscillations in the width and height.

Linewidth	50 nm	100 nm	200 nm
Modes (GHz)	1.360	1.672	1.411
	2.104	2.013	1.422
	3.284	3.001	2.16
	4.214	3.085	2.35
	5.034	3.578	2.767
	5.892	4.181	2.831

Table 1. Modelled resonant acoustic modes of imprinted polymer lines

This use of the photoacoustic method opens up the possibility of studying nanostructures' shapes and physical parameters, such as Young's modulus, without the need to focus the probe excitation, for example by using an AFM cantilever tip [14].

4 Conclusions

Photoacoustic metrology presents great potential as a characterisation tool for nanoimprinted structures. The photoacoustic method has been shown to be applicable to nanoimprint polymers having thicknesses of up to 600 nm. A good signal was obtained from the boundaries of two polymers with aluminium and silicon layers, allowing the measurement of the layer thicknesses or physical properties of the polymers, by using the time of flight data and simulations to make a full interpretation of the results. Simulations show that nanoscale imprinted polymer structures have acoustic resonant modes suitable for detection by photoacoustic microscopy.

Acknowledgements

The authors would like to acknowledge the work of Maryna Lishchynska of the Tyndall National Institute on finite element simulations of acoustic resonant modes.

The support of the EC-funded projects NaPa (Contract No. NMP4-CT-2003-500120), and of Science Foundation Ireland and are gratefully acknowledged. The content of this work is the sole responsibility of the authors.

References

[1] Chou S Y, Krauss P R and Renstrom P J "Imprint of sub-25 nm vias and trenches in polymers", *Applied Physics Letters* **67** (21), 3114-16 (1995)

[2] Chou S Y, and Krauss P R "Imprint Lithography with Sub-10 nm Feature Size and High Throughput", *Microelectronic Engineering* **35,** 237-40 (1997)

[3] Austin M D, Zhang W, Ge H, Wasserman D, Lyon S A and Chou S Y "6 nm half-pitch lines and 0.04 μm^2 static random access memory patterns by nanoimprint lithography", *Nanotechnology* **16,** 1058–61 (2005)

[4] Gourgon C, et al "Benchmarking in thermal nanoimprinting of 50 nm features", *J Vac Sci Technol B*. **25** (6), 2373-2378 (2007)

[5] Wu C W, Yamauchi Y, Ohsuna T and Kuroda K "Structural study of highly ordered mesoporous silica thin films and replicated Pt nanowires by high-resolution scanning electron microscopy", *Journal of Materials Chemistry* **16,** 3091-8 (2006)

[6] Giessibl J, "Atomic force microscopy's path to atomic resolution", *Materials Today* **8,** 32-41 (2005)

[7] Rasmussen A, and Deckert V "New dimension in nano-imaging: breaking through the diffraction limit with scanning near-field optical microscopy", *Analytical and Bioanalytical Chemistry* **381,** 165-72 (2005)

[8] 19. Smaali R, Fuard D, Perret C and Schiavone P 2005 Using scatterometry for 3D-feature metrology: application to Nano-Imprint Lithography Proc. of Nanoprint Nanoimprint Technology Conf. (October 2005, Nara, Japan) pp 32-3.

[9] Kehoe T, Bryner J, Reboud V, Kehagias N, Landis S, Gourgon C, Vollmann J, Dual J, Sotomayor Torres C.M., Sub-wavelength optical diffraction and photoacoustic metrologies for the characterisation of nanoimprinted structures, Proc. of SPIE Vol. 6921, 69210F1-9, 2008

[10] J. Vollmann, D. M. Profunser, and J. Dual. "Sensitivity improvement of a pump-probe set-up for thin film and microstructure metrology" *Ultrasonics*, 40(1-8), 757–763 (2002)

[11] C. Thomsen, H. T. Grahn, H. J. Maris, and J. Tauc. "Surface generation and detection of phonons by picosecond light-pulses", *Physical Review B* 34(6), 4129–4138, (1986).

[12] T. Q. Qiu ,and C. L. Tien. "Short-pulse laser-heating on metals", *International Journal of Heat and Mass Transfer*, 35(3), 719–726 (1992)

[13] T. Bienville, J.F. Robillard, L. Belliard, I. Roch-Jeune, A. Devos, B. Perrin, Individual and collective vibrational modes of nanostructures studied by picosecond ultrasonics, Ultrasonics 44 (2006) e1289–e1294

[14] D.M. Profunser, J. Vollmann, J. Dual, Ultrasonic wave propagation in focussing tips with arbitrary geometries, Ultrasonics 40 (2002) 747–752